

# REMOVALNET: DNN Fingerprint Removal Attacks

Hongwei Yao, Zheng Li, Kunzhe Huang, Jian Lou, Zhan Qin <sup>†</sup>, and Kui Ren, *Fellow, IEEE*

**Abstract**—With the performance of deep neural networks (DNNs) remarkably improving, DNNs have been widely used in many areas. Consequently, the DNN model has become a valuable asset, and its intellectual property is safeguarded by ownership verification techniques (e.g., DNN fingerprinting). However, the feasibility of the DNN fingerprint removal attack and its potential influence remains an open problem. In this paper, we perform the first comprehensive investigation of DNN fingerprint removal attacks. Generally, the knowledge contained in a DNN model can be categorized into general semantic and fingerprint-specific knowledge. To this end, we propose a min-max bilevel optimization-based DNN fingerprint removal attack named REMOVALNET, to evade model ownership verification. The lower-level optimization is designed to remove fingerprint-specific knowledge. While in the upper-level optimization, we distill the victim model's general semantic knowledge to maintain the surrogate model's performance. We conduct extensive experiments to evaluate the **fidelity**, **effectiveness**, and **efficiency** of the REMOVALNET against four advanced defense methods on six metrics. The empirical results demonstrate that (1) the REMOVALNET is **effective**. After our DNN fingerprint removal attack, the model distance between the target and surrogate models is  $\times 100$  times higher than that of the baseline attacks, (2) the REMOVALNET is **efficient**. It uses only 0.2% (400 samples) of the substitute dataset and 1,000 iterations to conduct our attack. Besides, compared with advanced model stealing attacks, the REMOVALNET saves nearly 85% of computational resources at most, (3) the REMOVALNET achieves high **fidelity** that the created surrogate model maintains high accuracy after the DNN fingerprint removal process. Our code is available at: <https://github.com/grasses/RemovalNet>.

**Index Terms**—DNN fingerprint removal, DNN fingerprinting, ownership verification.

## 1 INTRODUCTION

As the performance of deep neural networks (DNNs) remarkably improving, DNNs have been widely used in many areas (e.g., image recognition [1], [2] and natural language processing [3], [4]). However, training a high-performance DNN model requires tremendous training data and computational resources. Especially confidential datasets (e.g., medical, biological data, and facial images) are collected and protected by organizations that are reluctant to open-source. In this practical context, the DNN model becomes a valuable asset, which prompts the adversary to steal the victim model instead of constructing a model from scratch [5], [6], [7], [8].

Recently, many ownership verification techniques have been proposed to protect the intellectual property (IP) of the DNN models. Given a victim model and a suspected model, the ownership verification algorithm aims to determine whether the suspected model is derived from the victim model. Depending on the verification strategy, the DNN ownership verification algorithms can be broadly

categorized into watermarking and fingerprinting. DNN watermarking [9], [10], [11], [12], [13], [14], [15] is an active ownership verification technology that actively embeds an imperceptible watermark (e.g., noise or trigger pattern) into the redundant weights of the victim model. During the evaluation phase, the stealing action can be detected if a similar watermark can be extracted from the suspected model. Different from watermarking, DNN fingerprinting [16], [17], [18], [19], [20], [21], [22], [23], [24] is a passive ownership verification technology. DNN fingerprinting is non-invasive in that it only extracts a sequence of probing samples (i.e., fingerprints) from the victim model without modifying the model itself. During the verification phase, the verifier traces the behavioral patterns of the DNN model using the extracted probing samples. DNN fingerprinting leaves the victim model unaltered, whereas watermarking involves modifying it.

On the other hand, consider a *post-stealing* scenario, i.e., ownership verification attacks. After stealing from the victim model, the adversary utilizes the victim model to derive a surrogate model, attempting to bypass ownership verification systems. In most literature of current studies, the attackers focus on detecting and removing watermarks on the DNN model [25], [26], [27], [28]. However, the feasibility of DNN fingerprint removal is still an open problem, and understanding whether DNN fingerprinting can suffer from such removal attacks is a pressing question. DNN fingerprint removal attacks undermine the confidentiality and reliability of ownership verification algorithms, causing a loss of trust and confidence in the system. Removing the DNN fingerprint from the victim model while maintaining its performance involves three key challenges. Firstly, fin-

- Kui Ren and Zhan Qin are with School of Cyber Science and Technology, Zhejiang University, and Zhejiang Provincial Key Laboratory of Blockchain and Cyberspace Governance, Hangzhou, China. Zhan Qin is the corresponding author. (E-mail: [kuiren@zju.edu.cn](mailto:kuiren@zju.edu.cn) and [qinzhao@zju.edu.cn](mailto:qinzhao@zju.edu.cn)).
- Jian Lou is with ZJU-Hangzhou Global Scientific and Technological Innovation Center, Hangzhou, China. (E-mail: [jian.lou@zju.edu.cn](mailto:jian.lou@zju.edu.cn))
- Zheng Li is with the German National Big Science Institution within the Helmholtz Association, Saarbrücken, German (E-mail: [zheng.li@cispa.de](mailto:zheng.li@cispa.de)).
- Hongwei Yao and Kunzhe Huang are with School of Cyber Science and Technology, Zhejiang University, Hangzhou, China. (E-mail: [yhongwei@zju.edu.cn](mailto:yhongwei@zju.edu.cn) and [hkunzhe@zju.edu.cn](mailto:hkunzhe@zju.edu.cn)).

gerprints are intrinsic characteristics of the DNN models, which are deeply embedded in the neurons. However, a sophisticated DNN contains billions of neurons that interact with each other. Therefore, it's a challenge to devise an effective algorithm to remove them. Secondly, since the neural network relies on extracted feature maps to perform desired functions, directly removing them will inevitably degrade the performance of the surrogate model. As a result, the second challenge for the adversary is to perform an effective attack while maintaining the utility of the surrogate model. Thirdly, while retraining the model can circumvent ownership verification, it can be a resource-intensive and time-consuming process, particularly when the attacker is unaware of the training data. In other words, the attacker should balance the trade-off between efficiency and effectiveness.

In this paper, we investigate the *post-stealing* scenario attacks and propose an optimization-based DNN fingerprint removal attack REMOVALNET. We categorize the knowledge of DNNs includes general semantic knowledge and fingerprint-specific knowledge [29]. General semantic knowledge is relevant to the main task of the model, which controls the model's accuracy. On the other hand, fingerprint-specific knowledge originates from intrinsic characteristics of the DNN model, which is reflected as a sequence of behavioral patterns on latent representations and decision boundaries. The key idea of our method is to extract the general semantic knowledge of the victim model and progressively delete its behavioral patterns. In particular, we propose a min-max bilevel optimization algorithm to remove the fingerprint of the victim model. Specifically, in the lower-level problem, we intend to fine-tune a surrogate model that behaves differently from the victim model (e.g., layer outputs and activated neurons) but expresses similar semantic meaning. In contrast, in the upper-level problem, we seek to learn the victim model's general semantic knowledge to maintain its performance.

We conduct extensive experiments on five benchmark datasets (i.e., CIFAR10, GTSRB, Skin Lesion Diagnosis, CelebA, and ImageNet), including traffic sign recognition, disease diagnosis, face recognition, and large-scale visual recognition scenarios. The evaluation results demonstrate that the proposed REMOVALNET effectively and efficiently removes the DNN fingerprint left on the latent representations and decision boundaries. The major contributions of this paper are summarized as follows:

- We perform the first systematic investigation on DNN fingerprint removal attacks and demonstrate that it poses immense threats to model copyright protection.
- We propose a min-max bilevel optimization-based DNN fingerprint removal attack. The REMOVALNET is primarily designed to remove the victim model's behavioral patterns on latent representations and decision boundaries.
- We conduct extensive experiments to evaluate the REMOVALNET across six metrics on five benchmark datasets. The evaluation results demonstrate that the REMOVALNET is effective and efficient in removing DNN fingerprints, meanwhile maintaining high ac-

curacy on the surrogate model.

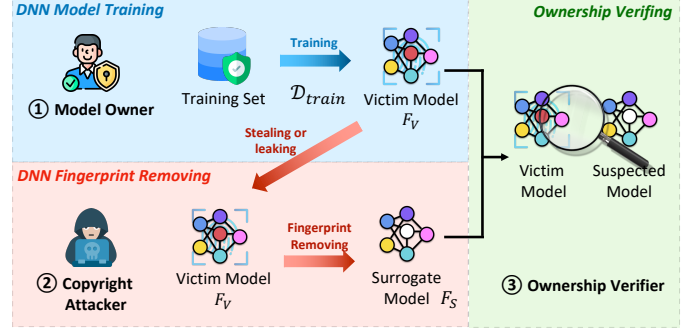


Fig. 1. Illustration of three roles in DNN ownership verification, a *model owner*, a *copyright attacker*, and an *ownership verifier*.

## 2 PRELIMINARIES

### 2.1 Problem Statement

A Deep Neural Network (DNN) model is a function  $F : \mathcal{X} \rightarrow \mathcal{Y}$  parameterized by a set of parameters  $\mathbf{w}$ , where  $\mathcal{X} \in \mathbb{R}^d$  is a  $d$ -dimensional input space and  $\mathcal{Y} \in \{1, 2, \dots, K\}$  represents a set of  $K$ -label. For the sake of convenience, we divide the original model  $F$  into two parts at the  $l$ -th layers, referring to as  $F^{l-}$  and  $F^{l+}$ , respectively. Therefore, the original model is denoted as  $F(x) = F^{l+} \circ F^{l-}(x)$ , where  $F^{l-}(x)$  represents the output of layer  $l$  ( $2 \leq l \leq L$ ).

### 2.2 Ownership Verification

In practice, we consider three roles in the problem of ownership verification, i.e., a *model owner*, a *copyright attacker*, and an *ownership verifier* (as illustrated in Figure 1). The model owner collects and utilizes training set  $\mathcal{D}_{train}$  to build his model  $F_V$  that achieves high accuracy on the test set  $\mathcal{D}_{test}$ . The adversary leverages the victim model to derive a surrogate model  $F_S$  aiming to break the ownership verification system. As a third party, the verifier has white-box access to both the victim model  $F_V$  and the suspected model  $F_S$ .

**DNN fingerprinting.** DNN fingerprinting relies on intrinsic characteristics of the neural network to verify whether the suspected model  $F_S$  is pirated of  $F_V$ . Those characteristics are the traces of training optimization, reflected as a sequence of unique model behavioral patterns for specific probing inputs (i.e., fingerprint data). Without loss of generality, a DNN fingerprinting algorithm consists of two phases: *fingerprint extraction* and *copyright verification*.

- **Fingerprint extraction:**  $E(F_V, \mathcal{D}_{train})$ . Given a victim model  $F_V$  and training data  $\mathcal{D}_{train}$ , outputs a number of  $N_{fp}$  fingerprints,  $\mathcal{D}_{fp} = E(F_V, \mathcal{D}_{train})$ .
- **Copyright verification:**  $V(F_V, F_S, \mathcal{D}_{fp}, d)$ . The copyright verification algorithm exploits lots of distance metrics as evidence to determine the results. Given a fingerprint set  $\mathcal{D}_{fp}$ , a distance metric  $d$  returns the average distance between  $F_V$  and  $F_S$ .

### 2.3 Model Distance Metrics

The advanced DNN fingerprinting methods typically rely on a set of distance metrics to establish evidence for ascertaining ownership of a suspected model. Specifically, those metrics can be categorized into the latent representation-based distance (e.g., DeepJudge [20], ZEST [21]) or decision boundary-based similarity (e.g., ModelDiff [23], IPGuard [18]). Additionally, those metrics compass a wide range of cutting-edge techniques, covering white-box and black-box defense strategies. We will describe those metrics in the following paragraph.

**DeepJudge [20].** Chen *et al.* propose six metrics to measure the distance between two DNN models, which can be used as evidence for ownership verification. We select two representative metrics to evaluate our fingerprint removal attack, i.e., Layer Output Distance (LOD) and Layer Activation Distance (LAD). LOD measures the  $L_p$ -norm distance between the two models' layer outputs:

$$LOD(F_V, F_S, \mathcal{D}_{fp}) = \frac{1}{N_{fp}} \sum_{i=1}^{N_{fp}} \|F_V^l(x_i) - F_S^l(x_i)\|_p. \quad (1)$$

LAD measures the average distance of activation neurons for layer  $l$ :

$$LAD(F_V, F_S, \mathcal{D}_{fp}) = \frac{1}{N_l \times N_{fp}} \sum_{j=1}^{N_l} \sum_{i=1}^{N_{fp}} |\phi_T^{l,j}(x_i) - \phi_S^{l,j}(x_i)|, \quad (2)$$

where  $N_l$  denotes the number of neurons for  $l$ -th layer's feature maps,  $\phi_T^{l,i}$  returns 1 if the  $i$ -th neuron for the output of  $l$ -th layer greater than a certain threshold. Since the model distance computation is based on the output of intermediate layers, the two suspected models should have the same model architecture.

**ZEST [21].** Jia *et al.* leverage LIME [30] technique to approximate the global behavior of two models. ZEST first approximates the models on reference data with linear models trained by LIME. Subsequently, ZEST computes the L2 norm or cosine similarity on the trained models to quantitatively measure the distance between two suspected models.

**ModelDiff [23].** Li *et al.* propose Decision Distance Vector (DDV) to approximate the behavioral patterns of a model:

$$DDV_F(\mathcal{D}_{fp}) = \{ \|F(x_i) - F(x_j)\|_2 | 0 \leq i < j \leq N_{fp} \}. \quad (3)$$

Afterward, the knowledge similarity between two models is measured with the cosine similarity between their DDVs:

$$Sim(F_V, F_S) = \text{CosineSimilarity}(DDV_{F_V}, DDV_{F_S}). \quad (4)$$

**IPGuard [18].** IPGuard explores data points near the decision boundaries to fingerprint the boundary property of the victim model. In this context, Marching Rate (MR) is proposed as a metric to measure the degree of similarity between two models on the decision boundary:

$$MR = \frac{1}{N_{fp}} \sum_{i=1}^{N_{fp}} \mathbb{1} [\arg \max F_V(x_i) = \arg \max F_S(x_i)]. \quad (5)$$

It should be noted that both DeepJudge and ZEST return the distance between two models, while the ModelDiff and IPGuard return the similarity score of two models.

### 2.4 Threat Model

In this section, we formulate the threat model to characterize the adversary's goals and capabilities. We will first define

DNN fingerprint removal attacks.

**DNN fingerprint removal attacks.** Given a victim model  $F_V$  and a substitute set  $\mathcal{D}_{sub}$ , the adversary intends to derive a surrogate model  $F_S$  from  $F_V$ . The DNN fingerprint removal attacks are designed to purge fingerprint-specific knowledge of the victim model. After the removal procedure, the created surrogate model is expected to behave differently from the victim model (e.g., output distance or distribution of activated neurons or decision boundaries). The formal definition of DNN fingerprint removal attacks is given below:

**Definition 2.1** (DNN fingerprint removal). Given a victim model  $F_V$ , a fingerprint set  $\mathcal{D}_{fp}$ , a copyright verification method  $V$ , the surrogate model  $F_S$  is ( $\mathcal{D}_{fp}, d, \tau$ )-fingerprint removal if

$$\mathbb{E}_{x \sim \mathcal{D}_{fp}} [V(F_V, F_S, x, d)] > \tau, \quad (6)$$

where  $d$  denotes the distance metric,  $\tau$  is a threshold. Noted that the adversary can't access  $\mathcal{D}_{fp}$  but uses a substitute set  $\mathcal{D}_{sub}$  to conduct the removal procedure.

**Attack motivations.** We first list potential motivations for conducting the DNN fingerprint removal attack.

(1) *Breaking system reliability.* The adversary intends to derive a functionality-preserved surrogate model  $F_S$  from the victim model  $F_V$ , which obfuscates the defense algorithm and breaks the reliability of the ownership verification system. Besides, the removal attack should remarkably reduce the training resources (e.g., computational resources and data for training) compared with model retraining. Therefore, the adversary's goal falls into three categories, i.e., *fidelity*, *effectiveness*, and *efficiency*.

- **Fidelity:** The surrogate model should maintain the performance of the victim model on the  $\mathcal{D}_{test}$ . We adopt accuracy and accuracy drops to measure the fidelity of the surrogate model. Therefore, the goal of the adversary in fidelity can be summarized as follows:

$$\max_{F_S} P_{(x,y) \in \mathcal{D}_{test}} \mathbb{1} [\arg \max F_S(x) = y]. \quad (7)$$

- **Effectiveness:** The effectiveness metric describes the capability of DNN fingerprint removal attacks to evade ownership verification techniques. As a result, the goal of the adversary in effectiveness can be summarized as follows:

$$\max_{F_S} P_{x \in \mathcal{D}_{fp}} [V(F_V, F_S, x, d)]. \quad (8)$$

- **Efficiency:** In general, retraining a model can circumvent ownership verification completely. While retraining has proven successful, there is a trade-off between its effectiveness and efficiency. Generally, the cost of DNN fingerprint removal attacks should be remarkably lower than model retraining.

(2) *Understanding the capability of attack.* Except for the aforementioned malicious goal, we consider a more open-world scenario to evaluate the capability of DNN fingerprint attacks. Specifically, the adversary attempts to determine the minimum resources required to bypass a DNN ownership verification system, which also can be useful in evaluating

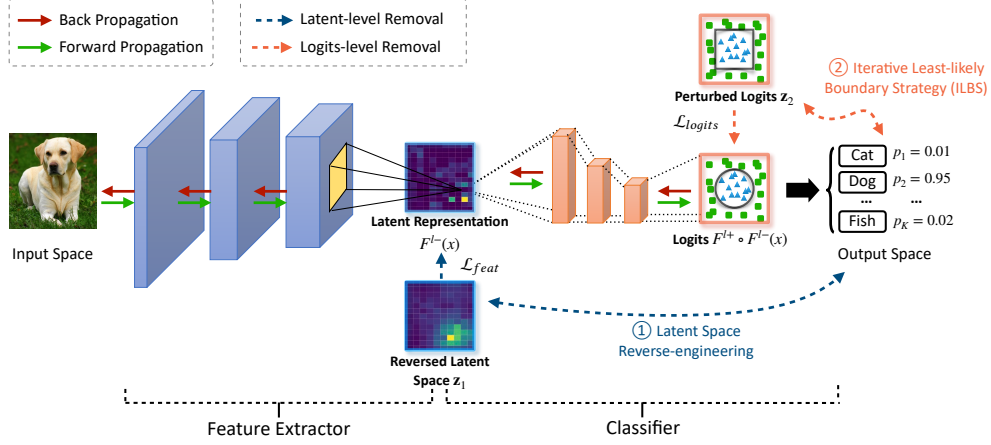


Fig. 2. Overview of REMOVALNET against DNN ownership verification. The removal process is conducted on the latent-level and logits-level to alter the behavior patterns in the latent representation and decision boundary, respectively.

the system’s overall robustness. Additionally, we suggest that DNN fingerprint removal attacks can be leveraged as a novel tool for evaluating the performance of ownership verification systems. For example, a confidential ownership verification system can utilize our algorithm to perform a comprehensive evaluation of its system before deployment, guaranteeing its effectiveness and security.

**Attacker’s capabilities.** Motivated by recent works in DNN watermark removal attacks [14], [26], [31], we make the assumption that the adversary has a limited substitute set  $\mathcal{D}_{sub}$  for fine-tuning. The substitute set assumption is a realistic assumption since many organizations or research communities have open-source plenty of benchmark datasets, part of which can be utilized as surrogate data. Specifically, we consider two scenarios of the adversary:

- **Limited Training Data ( $\mathcal{S}_{LTD}$ ).** The adversary only has access to a small part of training data (e.g., 10% of training data).
- **Limited Surrogate Data ( $\mathcal{S}_{LSD}$ ).** The adversary may acquire natural samples that share a similar distribution to the training set.

**Defender’s capabilities.** The defender has full access to both the victim model  $F_V$ , the suspected model  $F_S$ , and the fingerprint set  $\mathcal{D}_{fp}$ . The defender has unlimited computation resources to extract fingerprints and verify the ownership of the suspected models.

### 3 REMOVALNET

In this section, we present the detail of REMOVALNET, including substitute set selection, latent-level removal, and logits-level removal.

**Overall workflow.** Our approach involves dividing the neural network into two modules: a feature extractor that produces latent representations and a classifier that returns the logits vector. We propose removing DNN fingerprints at two levels: the latent-level and the logits-level, as depicted in Figure 2. The latent-level removal is intended to eliminate the behavior patterns in the representation layer, while the

logits-level removal alters the decision boundaries’ behavior patterns.

Firstly, we reverse the latent layer from the victim model and inject perturbation into it:

$$\{\mathbf{z}_1, \mathbf{z}_2\} = \{F_V^{l-}(x) + \delta_1, F_V^{l+} \circ F_V^{l-}(x) + \delta_2\}, \quad (9)$$

where  $\delta_1$  and  $\delta_2$  perturb on the latent representation layer  $l$  and the penultimate layer, respectively. Secondly, we minimize the distance between  $\{\mathbf{z}_1, \mathbf{z}_2\}$  and the surrogate model’s corresponding outputs. Subsequently, the behavioral patterns of the victim model will progressively be removed from the surrogate model.

The removal procedure can be formulated as a min-max bilevel optimization problem. In our method, the lower-level problem is to find a layer output that behaves differently from the victim model but has a similar semantic meaning. This process is conducted by maximizing the distance of latent representation between the target and surrogate models. In contrast, the upper-level problem involves distilling the reversed layer output while minimizing the loss of the main task to prevent catastrophic forgetting. Specifically, given a loss function  $\mathcal{L}$ , the optimal surrogate model  $F_S$  can be optimized by empirical risk:

$$\begin{aligned} \mathbf{w} &= \min_{\mathbf{w}} \max_{\mathbf{z}} \mathcal{L}(\mathbf{w}, \{\mathbf{z}^*\}; \mathcal{D}_{sub}), \\ s.t. & \arg \max F_S^{l+}(\mathbf{z}^*) = \arg \max F_V^{l+}(\mathbf{z}^*), \end{aligned} \quad (10)$$

where  $\mathbf{w}$  is the parameters of surrogate model  $F_S$ ,  $\mathbf{z}$  denotes the output of selected layer  $l$ . Figure 2 schematically illustrates the framework of REMOVALNET.

#### 3.1 Substitute Set Selection

As described in Definition 2.1, the DNN ownership is validated on the fingerprint set  $\mathcal{D}_{fp}$ . However, the DNN fingerprint set is generated and safeguarded by the verifier. Therefore, the first step toward the DNN fingerprint removal attacks is to select the substitute set  $\mathcal{D}_{sub}$ .

The selection of the substitute set should adhere to two key principles: (1) diversity in classes and (2) similarity in data distribution. The ownership verification algorithms are usually designed by measuring the distances between

the target and surrogate models over different classes. To enhance the performance of removal attacks, we tend to select substitute data with diverse classes. Additionally, to avoid the risk of catastrophic forgetting, we choose natural samples that reflect a similar distribution to the training set. Note that we only use a small number of substitute data, which can collect from the public benchmark datasets. We also discuss the confidential scenario in Section 4.4.1, where it's hard to collect the substitute data.

### 3.2 Latent-level Removal

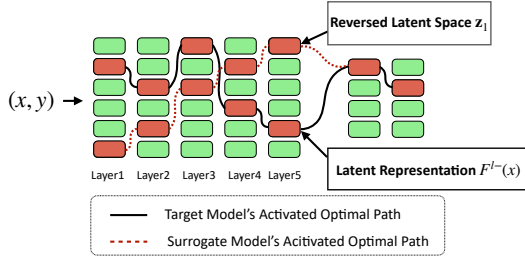


Fig. 3. DNN fingerprint removal attack on latent-level. The reversed latent space follows a logic similar to the victim model but triggers an alternative path.

The artificial neural network expresses logic using a sequence of activated neurons that output values higher than the threshold [32]. Since the activation status of neurons is highly related to the learning objective and learning progress, it can be exploited to measure the model distance. Therefore, the activation status of neurons plays an important role in DNN fingerprinting. Then we would ask whether we can find an optimal path that activates a set of neurons different from the victim model. Recent works on mitigating catastrophic forgetting have investigated the possibility of finding another optimal path for new tasks [33], [34]. Those works exploit the redundant weights of neural networks to activate a different set of neurons (as illustrated in Figure 3).

---

#### Algorithm 1: Latent space reverse-engineering

---

**Input:** victim model  $F_V$ , surrogate model  $F_S$ , selected layer  $l$ ,  $F_V$ 's first  $l$  layer output  $F_V^{l-}$ ,  $F_V$ 's last  $l$  layer output  $F_V^{l+}$ , substitute data  $(x, y) \in \mathcal{D}_{sub}$ , learning rate  $\eta$ .

**Output:** Feature maps hyperplane  $\mathbf{z}_1$

```

1  $\mathbf{z}'_1 = F_V^{l-}(x)$ 
2  $\hat{y} = \arg \max F_V(x)$ 
3 for  $i \leftarrow 1$  to 10 do
4    $\mathbf{z}_1 = \text{Feature\_Shuffling}(\mathbf{z}_1, \text{ratio} = 0.1)$ 
5    $\mathcal{L}_{re} = \mathcal{L}_{CE}(F_S^{l+}(\mathbf{z}_1), \hat{y}) - \log \|\mathbf{z}_1 - \mathbf{z}'_1\|_2$ 
6    $\mathbf{z}_1 = \mathbf{z}_1 - \eta \cdot \frac{\partial \mathcal{L}_{re}}{\partial \mathbf{z}_1}$ 
7 end
8 return  $\mathbf{z}_1$ 

```

---

Based insight mentioned above, we propose the latent-level fingerprint removal attack. The first step toward latent-level fingerprint removal is to reverse a detached latent space  $\mathbf{z}_1$ . Similar to reverse engineering in the input space,

we reverse the latent space hyperplane  $\mathbf{z}_1$  with two constraints: (1) adopt cross-entropy to make  $\mathbf{z}_1$  have similar semantic logic as  $F_V^{l-}(x)$ , (2) maximize the distance between  $\mathbf{z}_1$  and  $F_V^{l-}(x)$  (as illustrated in the line 5 of Algorithm 1). To enhance diversity during optimization, we employ feature shuffling on the reversed latent representation, which is inspired by recent works on data transformation (line 4 of Algorithm 1).

In contrast, in the upper-level problem, we optimize the following loss function:

$$\mathcal{L}_{feat} = \|F_S^{l-}(x) - \mathbf{z}_1\|_2. \quad (11)$$

Finally, we project the reversed latent space  $\mathbf{z}_1$  on the upper-level problem using the following objective function:

$$\begin{aligned} \mathbf{w} = \min_{\mathbf{w}} \max_{\mathbf{z}_1^*} \mathcal{L}_{feat} \\ \text{s.t. } \arg \max F_S^{l+}(\mathbf{z}_1^*) = \arg \max F_V(x). \end{aligned} \quad (12)$$

---

#### Algorithm 2: Iterative least-likely boundary strategy

---

**Input:** victim model  $F_V$ , a batch of substitute data

$\mathcal{B} \in \mathcal{D}_{sub}$ .

**Output:** Perturbed logits  $\mathbf{z}_B$

```

1  $\mathbf{z}_B = \{\}, id_{x_B} = \{\}$ 
2 // Find the indexes of the greatest distance samples
3 for  $i \leftarrow 1$  to  $|\mathcal{B}|$  do
4    $(x_i, y_i) = \mathcal{B}[i]$ 
5    $d_{max} = 0, id_{x_{max}} = i$ 
6   for  $j \leftarrow 1$  to  $|\mathcal{B}|$  do
7      $(x_j, y_j) = \mathcal{B}[j]$ 
8     if  $d_{max} < \|F_V(x_i) - F_V(x_j)\|_2$  then
9        $d_{max} = \|F_V(x_i) - F_V(x_j)\|_2$ 
10       $id_{x_{max}} = j$ 
11     end
12   end
13    $id_{x_B}[i] = id_{x_{max}}$ 
14 end
15 // Interpolate the target logits to maximize the
    decision boundary deviation
16 for  $i \leftarrow 1$  to  $|\mathcal{B}|$  do
17    $j = id_{x_B}[i]$ 
18    $(x_i, y_i) = \mathcal{B}[i]$ 
19   // Line search to find the optimal  $\lambda$ 
20   for  $\lambda = \{0.1, 0.2, \dots, 1.0\}$  do
21      $\mathbf{z}_2 = \lambda \cdot F_V(x_i) + (1 - \lambda) \cdot F_V(x_j)$ 
22     if  $\arg \max \mathbf{z}_2 = \arg \max F_V(x)$  then
23        $\mathbf{z}_B[i] = \mathbf{z}_2$ 
24     end
25   end
26 end
27 return  $\mathbf{z}_B$ 

```

---

### 3.3 Logits-level Removal

Generally, the natural sample is situated close to the center of its respective class, maintaining a significant distance

TABLE 1

Performance of REMOVALNET against DNN ownership verification. Large is better for DeepJudge and ZEST, while small is better for ModelDiff and IPGuard. “DJ-LOD” denotes the LOD metric of DeepJudge.

| Dataset                      | Attack Model      | Fidelity (%)                     |                   | Distance ( $\uparrow$ better)    |                                  |                                   |                                 | Similarity ( $\downarrow$ better) |                                   | Ownership?  |
|------------------------------|-------------------|----------------------------------|-------------------|----------------------------------|----------------------------------|-----------------------------------|---------------------------------|-----------------------------------|-----------------------------------|-------------|
|                              |                   | $F_S$                            | Drop $\downarrow$ | DJ-LOD                           | DJ-LAD                           | ZEST-L2                           | ZEST-Cosine                     | ModelDiff-DDV                     | IPGuard-MR                        |             |
| CIFAR10<br>(Acc: 90.58%)     | FT(0.5)           | 88.21 $\pm$ 0.31                 | 2.05              | 0.01 $\pm$ 0.02                  | 0.04 $\pm$ 0.03                  | 0.76 $\pm$ 0.14                   | 0.01 $\pm$ 0.01                 | 0.998 $\pm$ 0.002                 | 0.885 $\pm$ 0.020                 | Yes (10/10) |
|                              | FT(0.8)           | 87.22 $\pm$ 0.54                 | 3.03              | 0.02 $\pm$ 0.02                  | 0.04 $\pm$ 0.04                  | 1.03 $\pm$ 0.15                   | 0.01 $\pm$ 0.01                 | 0.997 $\pm$ 0.003                 | 0.875 $\pm$ 0.031                 | Yes (10/10) |
|                              | WP(0.5)           | 87.25 $\pm$ 0.63                 | 4.03              | 0.01 $\pm$ 0.02                  | 0.04 $\pm$ 0.02                  | 2.84 $\pm$ 0.47                   | 0.01 $\pm$ 0.01                 | 0.993 $\pm$ 0.001                 | 0.875 $\pm$ 0.073                 | Yes (10/10) |
|                              | WP(0.8)           | 85.27 $\pm$ 0.63                 | 5.21              | 0.02 $\pm$ 0.03                  | 0.05 $\pm$ 0.02                  | 14.04 $\pm$ 0.49                  | 0.02 $\pm$ 0.01                 | 0.943 $\pm$ 0.027                 | 0.844 $\pm$ 0.031                 | Yes (10/10) |
|                              | Distill           | 86.37 $\pm$ 0.56                 | 4.05              | 0.04 $\pm$ 0.03                  | 0.03 $\pm$ 0.02                  | 8.28 $\pm$ 4.96                   | 0.02 $\pm$ 0.01                 | 0.930 $\pm$ 0.022                 | 0.885 $\pm$ 0.166                 | Yes (10/10) |
|                              | Ours( $S_{LTD}$ ) | <u>87.17<math>\pm</math>1.75</u> | <u>2.89</u>       | <u>12.62<math>\pm</math>3.60</u> | <u>5.11<math>\pm</math>0.69</u>  | <u>115.86<math>\pm</math>2.71</u> | <u>0.51<math>\pm</math>0.03</u> | <u>0.321<math>\pm</math>0.140</u> | <u>0.061<math>\pm</math>0.043</u> | No (0/10)   |
|                              | Ours( $S_{LSD}$ ) | <u>86.81<math>\pm</math>2.24</u> | <u>3.23</u>       | <u>8.42<math>\pm</math>0.41</u>  | <u>5.51<math>\pm</math>0.69</u>  | <u>101.86<math>\pm</math>4.42</u> | <u>0.52<math>\pm</math>0.12</u> | <u>0.211<math>\pm</math>0.162</u> | <u>0.002<math>\pm</math>0.022</u> | No (0/10)   |
|                              | Negative          | 86.69 $\pm$ 1.08                 | 3.75              | 10.72 $\pm$ 2.00                 | 4.99 $\pm$ 0.90                  | 90.76 $\pm$ 3.09                  | 0.40 $\pm$ 0.02                 | 0.325 $\pm$ 0.231                 | 0.010 $\pm$ 0.021                 | No (0/10)   |
|                              | $\tau$            | -                                | -                 | 6.49                             | 2.95                             | 75.12                             | 0.319                           | 0.450                             | 0.250                             | -           |
| GTSRB<br>(Acc: 92.26%)       | FT(0.5)           | 94.03 $\pm$ 0.25                 | 0.25              | 3.23 $\pm$ 0.26                  | 0.28 $\pm$ 0.01                  | 8.78 $\pm$ 0.87                   | 0.01 $\pm$ 0.01                 | 0.959 $\pm$ 0.029                 | 0.857 $\pm$ 0.071                 | Yes (10/10) |
|                              | FT(0.8)           | 93.16 $\pm$ 0.30                 | 1.03              | 3.40 $\pm$ 0.26                  | 0.28 $\pm$ 0.01                  | 10.60 $\pm$ 1.08                  | 0.01 $\pm$ 0.00                 | 0.958 $\pm$ 0.029                 | 0.857 $\pm$ 0.143                 | Yes (10/10) |
|                              | WP(0.5)           | 92.94 $\pm$ 0.43                 | 1.25              | 3.69 $\pm$ 0.24                  | 0.38 $\pm$ 0.01                  | 16.19 $\pm$ 0.77                  | 0.03 $\pm$ 0.00                 | 0.935 $\pm$ 0.031                 | 0.857 $\pm$ 0.143                 | Yes (10/10) |
|                              | WP(0.8)           | 92.01 $\pm$ 0.82                 | 2.16              | 3.97 $\pm$ 0.31                  | 0.22 $\pm$ 0.01                  | 19.34 $\pm$ 2.88                  | 0.13 $\pm$ 0.01                 | 0.576 $\pm$ 0.112                 | 0.429 $\pm$ 0.286                 | Yes (10/10) |
|                              | Distill           | 91.78 $\pm$ 1.64                 | 2.23              | 3.44 $\pm$ 0.27                  | 0.27 $\pm$ 0.02                  | 21.74 $\pm$ 3.11                  | 0.07 $\pm$ 0.02                 | 0.489 $\pm$ 0.186                 | 0.714 $\pm$ 0.071                 | Yes (10/10) |
|                              | Ours( $S_{LTD}$ ) | <u>91.88<math>\pm</math>1.67</u> | <u>2.01</u>       | <u>11.20<math>\pm</math>0.05</u> | <u>19.92<math>\pm</math>0.30</u> | <u>137.01<math>\pm</math>0.12</u> | <u>0.63<math>\pm</math>0.04</u> | <u>0.115<math>\pm</math>0.146</u> | <u>0.251<math>\pm</math>0.143</u> | No (0/10)   |
|                              | Ours( $S_{LSD}$ ) | <u>92.02<math>\pm</math>0.75</u> | <u>2.15</u>       | <u>11.19<math>\pm</math>0.04</u> | <u>19.77<math>\pm</math>0.21</u> | <u>135.12<math>\pm</math>0.05</u> | <u>0.65<math>\pm</math>0.01</u> | <u>0.118<math>\pm</math>0.114</u> | <u>0.286<math>\pm</math>0.214</u> | No (0/10)   |
|                              | Negative          | 92.12 $\pm$ 1.88                 | 2.18              | 9.05 $\pm$ 1.18                  | 15.99 $\pm$ 1.10                 | <b>138.21<math>\pm</math>9.19</b> | 0.59 $\pm$ 0.11                 | 0.132 $\pm$ 0.243                 | <b>0.242<math>\pm</math>0.021</b> | No (0/10)   |
|                              | $\tau$            | -                                | -                 | 6.02                             | 13.26                            | 92.13                             | 0.40                            | 0.293                             | 0.472                             | -           |
| Skin Lesion<br>(Acc: 98.81%) | FT(0.5)           | 96.90 $\pm$ 0.14                 | 2.06              | 0.05 $\pm$ 0.01                  | 0.03 $\pm$ 0.01                  | 1.84 $\pm$ 0.10                   | 0.02 $\pm$ 0.01                 | 0.982 $\pm$ 0.001                 | 0.902 $\pm$ 0.009                 | Yes (10/10) |
|                              | FT(0.8)           | 95.72 $\pm$ 0.24                 | 3.16              | 0.08 $\pm$ 0.02                  | 0.04 $\pm$ 0.03                  | 2.34 $\pm$ 0.14                   | 0.11 $\pm$ 0.03                 | 0.958 $\pm$ 0.004                 | 0.915 $\pm$ 0.012                 | Yes (10/10) |
|                              | WP(0.5)           | 96.80 $\pm$ 0.15                 | 2.15              | 0.07 $\pm$ 0.06                  | 0.06 $\pm$ 0.01                  | 5.10 $\pm$ 0.08                   | 0.04 $\pm$ 0.01                 | 0.995 $\pm$ 0.003                 | 0.853 $\pm$ 0.011                 | Yes (10/10) |
|                              | WP(0.8)           | 95.64 $\pm$ 0.13                 | 4.31              | 0.10 $\pm$ 0.07                  | 0.07 $\pm$ 0.03                  | 12.09 $\pm$ 2.24                  | 0.02 $\pm$ 0.01                 | 0.957 $\pm$ 0.014                 | 0.856 $\pm$ 0.062                 | Yes (10/10) |
|                              | Distill           | 95.01 $\pm$ 0.41                 | 4.06              | 0.08 $\pm$ 0.02                  | 0.06 $\pm$ 0.02                  | 10.35 $\pm$ 2.02                  | 0.14 $\pm$ 0.02                 | 0.951 $\pm$ 0.005                 | 0.849 $\pm$ 0.048                 | Yes (10/10) |
|                              | Ours( $S_{LTD}$ ) | <u>97.29<math>\pm</math>0.42</u> | <u>1.21</u>       | <u>9.58<math>\pm</math>0.26</u>  | <u>3.99<math>\pm</math>1.05</u>  | <u>67.94<math>\pm</math>3.51</u>  | <u>0.48<math>\pm</math>0.12</u> | <u>0.159<math>\pm</math>0.125</u> | <u>0.164<math>\pm</math>0.044</u> | No (0/10)   |
|                              | Ours( $S_{LSD}$ ) | <u>94.35<math>\pm</math>1.38</u> | <u>3.34</u>       | <u>8.14<math>\pm</math>0.84</u>  | <u>3.32<math>\pm</math>0.63</u>  | <u>75.32<math>\pm</math>5.22</u>  | <u>0.54<math>\pm</math>0.12</u> | <u>0.152<math>\pm</math>0.156</u> | <u>0.161<math>\pm</math>0.036</u> | No (0/10)   |
|                              | Negative          | 98.58 $\pm$ 0.43                 | 0.25              | 9.57 $\pm$ 1.84                  | 4.09 $\pm$ 0.63                  | <b>86.27<math>\pm</math>9.22</b>  | 0.52 $\pm$ 0.07                 | 0.163 $\pm$ 0.039                 | <b>0.035<math>\pm</math>0.031</b> | No (0/10)   |
|                              | $\tau$            | -                                | -                 | 6.37                             | 2.72                             | 57.45                             | 0.35                            | 0.361                             | 0.405                             | -           |

from the decision boundary. In contrast, the extracted fingerprint data, often from adversarial inputs, tend to lie alongside the decision boundary. Therefore, it is possible to obfuscate the DNN fingerprinting verification by introducing deceptive non-robustness features. While these non-robustness features compromise the surrogate model’s robustness, they can effectively evade DNN fingerprinting verification. Specifically, we introduce a slight perturbation to the logits resulting in an altered decision boundary.

The critical challenge in logits-level removal is how to find the perturbed  $\mathbf{z}_2$ . To tackle this challenge, our paper introduces an iterative algorithm called the *iterative least-likely boundary strategy* (ILBS). Specifically, the proposed iterative strategy involves identifying pairs in a mini-batch with the greatest distance between logits. This is followed by the adoption of a linear interpolation logits vector to meet the imposed constraints. We rewrite the perturbed logits as  $F_V(x_i) + \delta_2 = \lambda F_V(x_i) + (1 - \lambda)F_V(x_j)$ , where  $x_j$  is the sample that has the greatest logits distance with  $x_i$ . Finally, we employ a line search strategy to find the best  $\lambda$  for the constraints. We illustrate the detail of ILBS in Algorithm 2. In lines 3-14 of Algorithm 2, we search the pairs with the greatest logits distance in a mini-batch. In lines 16-26 of Algorithm 2, we project the logits interpolation to maximize the decision boundary deviation. In lines 20-25 of Algorithm 2, we adopt the linear search to iteratively find the best  $\lambda$  that satisfies the constraint of  $\mathbf{z}_2$ .

Additionally, we adopt a cross-entropy loss on the logits-level removal to avoid catastrophic forgetting. Finally, the loss function can be formulated as:

$$\mathcal{L}_{logits} = \alpha \cdot \mathcal{L}_{CE}(F_V(x), \hat{y}) + (1 - \alpha) \cdot \mathcal{L}_{KL}(F_V(x), \mathbf{z}_2), \quad (13)$$

where  $\hat{y} = \arg \max F_V(x)$  is the predicted label. Then, we project the reversed logits  $\mathbf{z}_2$  on the upper-level problem using the following objective function:

$$\begin{aligned} \mathbf{w} &= \min_{\mathbf{w}} \max_{\mathbf{z}_2^*} \mathcal{L}_{logit} \\ &s.t. \arg \max_{\mathbf{z}_2^*} = \arg \max_{F_V(x)}. \end{aligned} \quad (14)$$

Finally, the loss function in Equation 10 can be rewritten as follows:

$$\mathcal{L} = \alpha \mathcal{L}_{CE} + (1 - \alpha) \mathcal{L}_{KL} + \beta \mathcal{L}_{feat}. \quad (15)$$

The latent-level and logits-level optimization are performed simultaneously during the min-max process.

To summarize, we eliminate the behavioral patterns of the DNN model at both the latent-level and logits-level. This is achieved by utilizing a min-max bilevel optimization paradigm, which enables us to preserve the model’s performance even after the fingerprints have been removed.

TABLE 2

Performance of REMOVALNET against DNN ownership verification. Large is better for DeepJudge and ZEST, while small is better for ModelDiff and IPGuard. “DJ-LOD” denotes the LOD metric of DeepJudge. “CelebA+20” and “CelebA+31” indicate the gender and smiling attributes of CelebA, respectively. ZEST fails to work for large model like ViT\_B/32.

| Dataset                    | Attack Model      | Fidelity (%)      |                   | Distance ( $\uparrow$ better) |                   |                   |                  | Similarity ( $\downarrow$ better) |                    | Ownership?  |
|----------------------------|-------------------|-------------------|-------------------|-------------------------------|-------------------|-------------------|------------------|-----------------------------------|--------------------|-------------|
|                            |                   | $F_S$             | Drop $\downarrow$ | DJ-LOD                        | DJ-LAD            | ZEST-L2           | ZEST-Cosine      | ModelDiff-DDV                     | IPGuard-MR         |             |
| CelebA+20<br>(Acc: 97.68%) | FT(0.5)           | 95.31±0.04        | 2.02              | 0.02±0.01                     | 0.01±0.01         | 1.55±0.53         | 0.01±0.01        | 0.991±0.002                       | 0.976±0.011        | Yes (10/10) |
|                            | FT(0.8)           | 94.23±0.07        | 3.12              | 0.03±0.02                     | 0.02±0.01         | 3.65±1.23         | 0.03±0.01        | 0.994±0.013                       | 0.967±0.017        | Yes (10/10) |
|                            | WP(0.5)           | 94.42±0.09        | 3.06              | 0.03±0.01                     | 0.06±0.03         | 4.62±1.03         | 0.03±0.02        | 0.990±0.011                       | 0.963±0.031        | Yes (10/10) |
|                            | WP(0.8)           | 93.04±0.07        | 4.20              | 0.04±0.03                     | 0.07±0.02         | 6.84±0.47         | 0.06±0.01        | 0.985±0.013                       | 0.952±0.023        | Yes (10/10) |
|                            | Distill           | 93.69±0.20        | 4.02              | 0.08±0.07                     | 0.23±0.10         | 7.20±1.23         | 0.05±0.02        | 0.960±0.025                       | 0.750±0.091        | Yes (10/10) |
|                            | Ours( $S_{LTD}$ ) | <u>94.18±5.91</u> | <u>1.42</u>       | <u>9.82±0.46</u>              | <u>6.30±1.16</u>  | <u>32.20±0.64</u> | <u>0.18±0.02</u> | <u>0.516±0.090</u>                | <u>0.299±0.073</u> | No (0/10)   |
|                            | Ours( $S_{LSD}$ ) | <u>94.30±3.21</u> | <u>3.59</u>       | <u>5.13±0.27</u>              | <u>7.51±1.89</u>  | <u>38.79±1.02</u> | <u>0.35±0.03</u> | <u>0.378±0.318</u>                | <u>0.247±0.172</u> | No (0/10)   |
|                            | Negative          | 96.71±0.47        | 0.94              | 7.69±2.03                     | 5.92±1.07         | 46.36±4.02        | 0.26±0.03        | 0.418±0.294                       | 0.039±0.015        | No (0/10)   |
|                            | $\tau$            | -                 | -                 | 5.14                          | 3.94              | 30.87             | 0.18             | 0.593                             | 0.410              | -           |
| CelebA+31<br>(Acc: 92.50%) | FT(0.5)           | 91.24±0.12        | 1.09              | 0.06±0.04                     | 0.07±0.03         | 1.27±0.21         | 0.01±0.01        | 0.991±0.012                       | 0.978±0.012        | Yes (10/10) |
|                            | FT(0.8)           | 90.17±0.11        | 2.07              | 0.07±0.05                     | 0.08±0.03         | 2.32±0.23         | 0.02±0.01        | 0.975±0.008                       | 0.944±0.020        | Yes (10/10) |
|                            | WP(0.5)           | 90.65±0.17        | 1.85              | 0.09±0.06                     | 0.09±0.04         | 2.64±0.12         | 0.02±0.01        | 0.989±0.013                       | 0.962±0.021        | Yes (10/10) |
|                            | WP(0.8)           | 90.21±0.23        | 2.28              | 0.10±0.08                     | 0.10±0.01         | 6.43±0.12         | 0.03±0.09        | 0.981±0.009                       | 0.951±0.008        | Yes (10/10) |
|                            | Distill           | 90.61±0.26        | 1.91              | 0.12±0.08                     | 0.25±0.04         | 7.42±0.67         | 0.02±0.01        | 0.963±0.005                       | 0.812±0.004        | Yes (10/10) |
|                            | Ours( $S_{LTD}$ ) | <u>90.65±2.12</u> | <u>1.70</u>       | <u>10.71±0.51</u>             | <u>13.48±0.08</u> | <u>31.23±2.41</u> | <u>0.40±0.09</u> | <u>0.204±0.162</u>                | <u>0.215±0.053</u> | No (0/10)   |
|                            | Ours( $S_{LSD}$ ) | <u>90.54±2.29</u> | <u>1.25</u>       | <u>6.57±0.31</u>              | <u>13.42±0.08</u> | <u>21.61±1.12</u> | <u>0.10±0.01</u> | <u>0.204±0.152</u>                | <u>0.173±0.022</u> | No (0/10)   |
|                            | Negative          | 91.83±0.30        | 0.62              | 5.89±1.68                     | 7.01±1.36         | 35.92±3.27        | 0.29±0.04        | 0.509±0.123                       | 0.016±0.019        | No (0/10)   |
|                            | $\tau$            | -                 | -                 | 3.78                          | 4.78              | 23.92             | 0.20             | 0.652                             | 0.405              | -           |
| ImageNet<br>(Acc: 71.13%)  | FT(0.5)           | 70.17±0.31        | 0.90              | 12.36±1.08                    | 0.62±0.15         | ×                 | ×                | 0.982±0.009                       | 0.815±0.120        | Yes (10/10) |
|                            | FT(0.8)           | 69.02±0.44        | 1.93              | 18.57±2.91                    | 1.70±1.23         | ×                 | ×                | 0.929±0.033                       | 0.766±0.084        | Yes (10/10) |
|                            | WP(0.5)           | 69.21±0.13        | 1.81              | 18.08±3.31                    | 7.34±3.83         | ×                 | ×                | 0.895±0.021                       | 0.641±0.107        | Yes (10/10) |
|                            | WP(0.8)           | 66.10±1.21        | 5.25              | 25.92±1.92                    | 9.30±2.82         | ×                 | ×                | 0.806±0.057                       | 0.579±0.101        | Yes (10/10) |
|                            | Distill           | 68.29±0.52        | 2.66              | 16.28±3.70                    | 3.21±0.43         | ×                 | ×                | 0.994±0.011                       | 0.626±0.062        | Yes (10/10) |
|                            | Ours( $S_{LTD}$ ) | <u>69.39±2.11</u> | <u>1.73</u>       | <u>142.26±5.69</u>            | <u>31.50±2.10</u> | ×                 | ×                | <u>0.248±0.203</u>                | <u>0.003±0.0</u>   | No (0/10)   |
|                            | Negative          | 64.57±0.28        | 6.57              | 134.76±7.58                   | 38.87±2.87        | ×                 | ×                | 0.353±0.055                       | 0.0±0.0            | No (0/10)   |
|                            | $\tau$            | -                 | -                 | 91.75                         | 25.89             | ×                 | ×                | 0.460                             | 0.201              | -           |

## 4 EXPERIMENTS

### 4.1 Experimental Setup

We evaluate REMOVALNET on five benchmark datasets, i.e., CIFAR10 [35], GTSRB [36], Skin Lesion Diagnosis [37], CelebA [38], and ImageNet [39], covering four scenarios, including traffic sign recognition, disease diagnosis, face recognition, and large-scale visual recognition. Noted that we adopt “CelebA+20” and “CelebA+31” to indicate the **gender** and **smiling** attributes of the CelebA dataset. All experiments run on an Ubuntu 20.04 system with 96-core Intel Xeon CPUs and 4 Nvidia GPUs of type GeForce GTX 3090. In the following context, we describe the generation of the negative, positive, and REMOVALNET models. Besides, we explain the defense methods and evaluation metrics in our experiments.

#### 4.1.1 Victim model selection

We run our experiments on five convolutional neural networks, including ResNet50, VGG19, DenseNet121, InceptionV3, and ViT (ViT\_B/32). For the input size of  $32 \times 32$ , we downsampled the filter size of the first convolutional layer in the original architecture. For the ImageNet task, the victim models are downloaded from the pre-trained repository of HuggingFace\*. Table 3 provides the summary of datasets and victim models used in our experiments.

\*<https://github.com/huggingface/pytorch-image-models>

TABLE 3

Datasets and victim models in experiments.

| Dataset       | Victim model | #Params | Accuracy(%) |
|---------------|--------------|---------|-------------|
| CIFAR10       | VGG19        | 38.96M  | 90.58       |
| GTSRB         | InceptionV3  | 21.64M  | 92.26       |
| Skin Lesion   | ResNet50     | 23.52M  | 98.81       |
| CelebA+20/+31 | DenseNet121  | 6.96M   | 97.68/92.50 |
| ImageNet      | ViT_B/32     | 88.19M  | 71.13       |

#### 4.1.2 Negative and positive models generation

Both positive, negative, and REMOVALNET models have the same model architecture as the victim model. In all of our experiments, we select ten random seeds, and the results are averaged over ten random tries.

**Negative models.** Negative models are trained on the same dataset as the victim model but have different random initializations. For ImageNet, we conduct our independent training from a pre-trained “ViT\_B/32\_sam” model. In order to simulate a real-world scenario, we randomly add a slight noise to the training iterations and learning rates for each group of random seeds.

**Positive models.** Four baseline attacks are considered in our experiments, including model fine-tuning, weight pruning, distillation, and model stealing. Both fine-tuning,

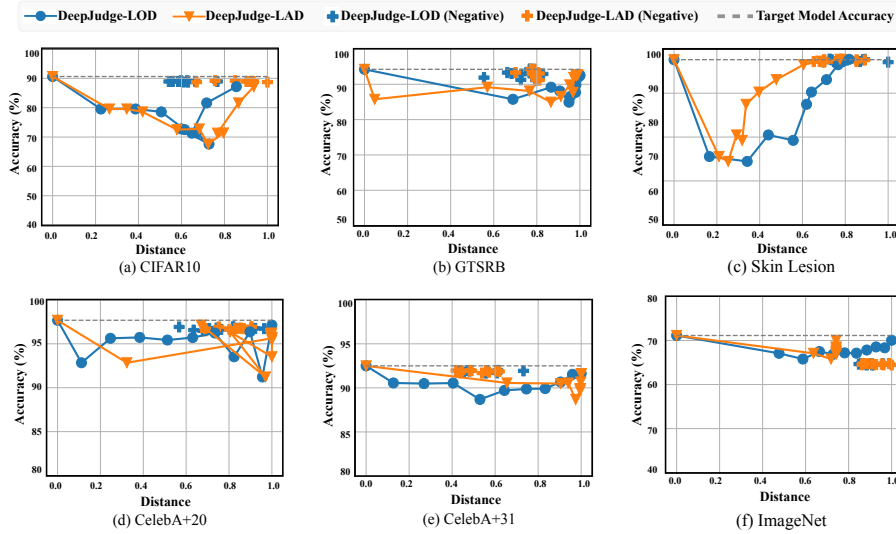


Fig. 4. The REMOVALNET attack vs. DeepJudge defense. Fidelity is presented on the  $y$ -axis and normalized model distance on the  $x$ -axis. The higher distance and fidelity of the surrogate model, the better performance of our attack.

weight pruning, and distillation are direct parameters reused from the victim model. For weight pruning, we first conduct the pruning process and then fine-tune 100 ~ 500 iterations on the surrogate model. For distillation, we distill the knowledge of the victim model using feature distillation. The model stealing attack is a pre-step of the DNN fingerprint removal attack, which also threatens the copyright of the victim model. We will investigate the comparison of efficiency between model stealing attacks and REMOVALNET in Section 4.4.2.

**REMOVALNET.** For both scenarios of  $S_{LTD}$  and  $S_{LSD}$ , we run our DNN fingerprint removal algorithm with 1000 iterations with a batch size of 128. The Stochastic Gradient Descent (SGD) optimizer with a momentum of 0.9 is adopted in our method. The surrogate datasets adopted in  $S_{LSD}$  for the tasks of CIFAR10, CelebA+20, CelebA+31, and Skin Lesion are CINIC10 [40], LFW [41], VGGFace2 [42], and BCN20000 [43], respectively. We divide the GTSRB dataset into two non-overlapping partitions and utilize only 15% of the training set as a surrogate dataset for  $S_{LSD}$ . We set  $\alpha = 0.2$ ,  $\beta = 2.0$ , and the learning rate to 0.01 as default hyper-parameters in our experiments. We will discuss the impact of the substitute dataset’s size in Section 4.4.1, and the impact of  $\alpha$ ,  $\beta$  in Section 4.5.

#### 4.1.3 Defense methods and copyright verification metrics

Four state-of-the-art defense methods (i.e., DeepJudge [20], ZEST [21], ModelDiff [23] IPGuard [18]), including 6+1 metrics, are considered in our experiments. The evaluation metrics can be categorized into two types: distance (DeepJudge-LOD, DeepJudge-LAD, ZEST-L2, and ZEST-Cosine) and similarity (ModelDiff-DDV and IPGuard-MR). We have explained the evaluation metrics in Section 2.3.

#### 4.1.4 Threshold selection

Due to the differences in statistical characteristics between various datasets and models, it is necessary to calculate the threshold ( $\tau$ ) beforehand. Similar to ModelDiff, we select a data-driven model-specific threshold. We independently

train several reference models that are similar to  $F_V$ . Subsequently, the threshold can be established as the highest similarity score or lowest distance score among those attained by the reference models.

## 4.2 Comparison with Baselines

In this section, we make a comparison of REMOVALNET with baseline attack methods, including fine-tuning, pruning, and distillation on six copyright verification metrics. We use Table 1 and Table 2 to evaluate the results of REMOVALNET on five benchmark datasets. In the column of “Fidelity,” we show the averaged accuracy and accuracy drop of the surrogate models. The columns “Distance” and “Similarity” illustrate the results of different surrogate models evaluated by various metrics. FT(0.5) denotes fine-tuning the last 50% of layers, and WP(0.5) means pruning 50% weights of the victim model. It should be noted that large is better for the “Distance” column, while small is better for the “Similarity” column. We underline the experimental results of REMOVALNET and bold the best results for each metric. Besides, our goal is not to achieve the best values but to obtain obfuscated results that can evade DNN fingerprinting algorithms.

Overall, the REMOVALNET remarkably outperforms all baseline attacks on all six metrics. Furthermore, the LOD and LAD results of REMOVALNET are  $\times 100$  times higher than that of the baseline attacks for most of the experiments, which are very close to the negative models. For example, in the CIFAR10 dataset, the REMOVALNET achieves  $9.82 \pm 0.64$  and  $5.13 \pm 0.27$  (for LOD metric), which is very close to  $7.69 \pm 0.23$  of negative models. Besides, the REMOVALNET also produces deceptive results on ModelDiff and IPGuard. For example, the REMOVALNET achieves  $0.159 \pm 0.125$  and  $0.152 \pm 0.156$  in ModelDiff-DDV for the Skin Lesion dataset, which is deceptive compared with  $0.163 \pm 0.039$  of negative models. Again, the matching rate (IPGuard) result of REMOVALNET on ImageNet is  $0.003 \pm 0.0$ , which is deceptive among negative models. On the other hand, the REMOVALNET evades the defense methods by only sacrificing slight



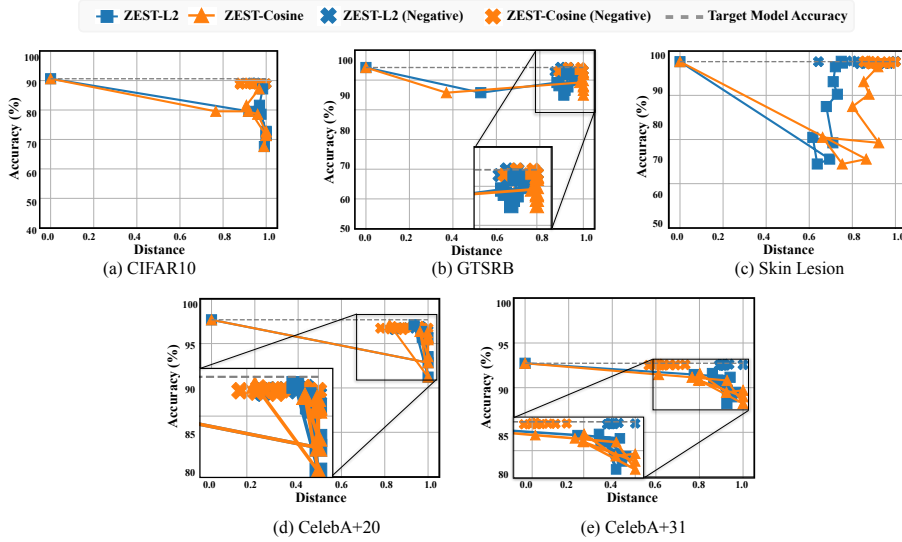


Fig. 5. The REMOVALNET attack vs. ZEST defense. Fidelity is presented on the  $y$ -axis and normalized model distance on the  $x$ -axis. The higher distance and fidelity of the surrogate model, the better performance of our attack.

fidelity drops. The largest fidelity drops are presented in the  $\mathcal{S}_{LSD}$  scenario of the Skin Lesion dataset (**small then 4% drops**). The reason behind this phenomenon is that the BCN20000's input distribution and the label space are quite different from the Skin Lesion dataset. Generally, the REMOVALNET is capable of sacrificing negligible accuracy drops to generate a surrogate model that can mislead the ownership verification algorithms.

### 4.3 Fidelity and Effectiveness of REMOVALNET

The trade-off between fidelity and effectiveness is a great challenge of DNN fingerprint removal attacks. In this section, we show the learning process of REMOVALNET to find the optimal surrogate model, which achieves high fidelity while removing the victim model's behavioral patterns. Figure 4 and Figure 5 depict the trade-off between the fidelity and attack performance of REMOVALNET. We sample every 100 iterations for REMOVALNET, with a total of 11 checkpoints (the first checkpoint is  $t = 0$ ). As illustrated in Figure 4 and Figure 5, the fidelity of the REMOVALNET first experiences a rapid decline, then progressively grows and finally reaches a stable value. The reason behind the fidelity rapid decline phenomenon is that the removal procedure over the latent-level and logits-level introduces the side effect of catastrophic forgetting. On the other hand, the results of DeepJudge and ZEST experienced a violent fluctuation during this period and finally reached a high value. Since the REMOVALNET has no knowledge of the DNN fingerprinting strategy and the fingerprint set, removing the behavioral patterns of the victim model is an indirect optimization process. As a result, the results of DeepJudge and ZEST fluctuate during this period. Although the fidelity of REMOVALNET has slight drops, we can sacrifice only a small fidelity to bypass the defense methods. In conclusion, the REMOVALNET attack is effective in removing the victim model's behavioral patterns and evading defense methods, only sacrificing little fidelity.

### 4.4 Efficiency of REMOVALNET

The efficiency of the DNN fingerprint removal attack contains two aspects: substitute set's size and computing resources (Section 2.4).

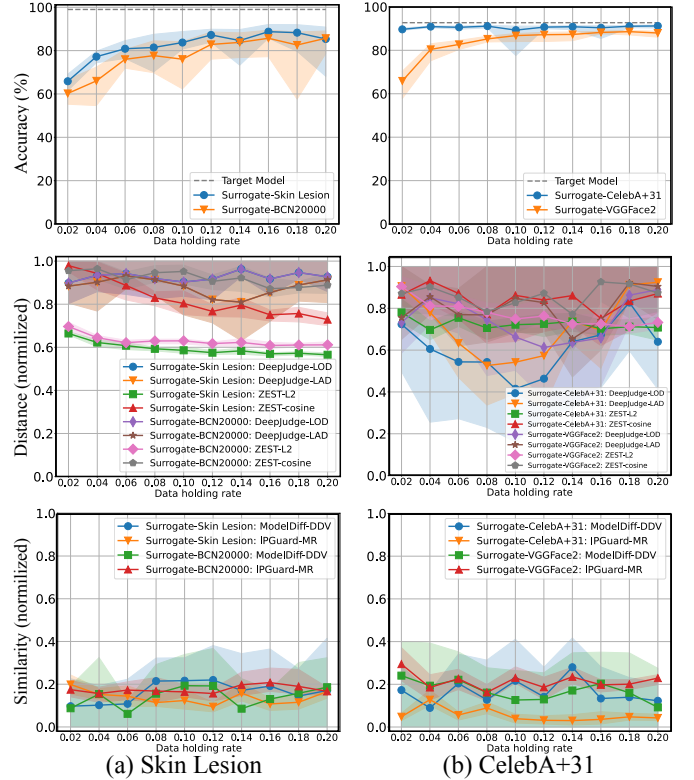


Fig. 6. The performance of REMOVALNET with different ratios of substitute data. The first to third rows show the fidelity, distance, and similarity that vary with the data holding rate.

#### 4.4.1 Substitute set's size.

In confidential scenarios (e.g., disease diagnosis and facial recognition), datasets are collected and protected by organi-

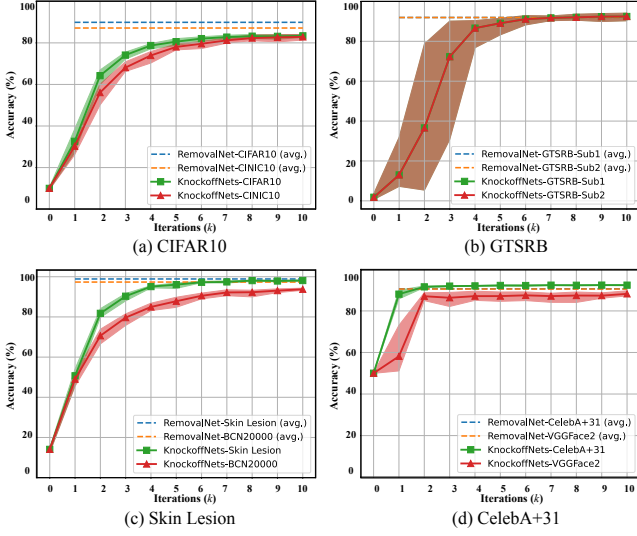


Fig. 7. The comparison of the computational efficiency between REMOVALNET (dashed line) and model stealing attacks (solid line).

zations. In this practical context, the substitute set’s size is critical to the utility of DNN fingerprint attacks.

For both  $\mathcal{S}_{LTD}$  and  $\mathcal{S}_{LSD}$  scenarios, we evaluate the performance of REMOVALNET under different ratios of substitute data (from 2% to 20%). In order to avoid catastrophic forgetting, we decrease the learning rate in this experiment. As illustrated in Figure 6, the REMOVALNET achieves higher fidelity with higher data holding ratios. However, the distance metric slightly decreases with higher data-holding ratios. This phenomenon is reasonable and within expectation. Since we adopt a lower learning rate, the optimizer tunes fewer weights and finally resulting in harder removing the behavioral patterns left in the victim model. It should be noted that for the Skin Lesions and VGGFace2 ( $p=2\%$ ) dataset (after Random Over-Sampling Examples, ROSE [44] labels rebalance), the adversary only holds 750 and 400 samples (saving 92.51% and 99.80% training data) to conduct the DNN fingerprint removal attack, respectively. Overall, even with a small ratio of substitute data, the REMOVALNET still has comparable fidelity and ownership verification evading capability.

#### 4.4.2 Computational resources

Till recently, there is still no DNN fingerprint removal attack that is comparable to REMOVALNET. Therefore, we have decided to use the model stealing attack as a benchmark to evaluate the computational resources required by REMOVALNET. In this context, we make a comparison of computation efficiency between REMOVALNET and model stealing attacks.

KnockoffNets [45] is an efficient model stealing attack which exploits the active learning paradigm to increase stealing efficiency. Similar to REMOVALNET, we consider  $\mathcal{S}_{LTD}$  and  $\mathcal{S}_{LSD}$  scenarios for KnockoffNets, and set the query budget to  $batch\_size \times 10000$  (10,000 iterations). Since there is no substitute dataset comparable to ImageNet, we only evaluate the efficiency between REMOVALNET and KnockoffNets on the CIFAR10, GTSRB, Skin Lesion, and

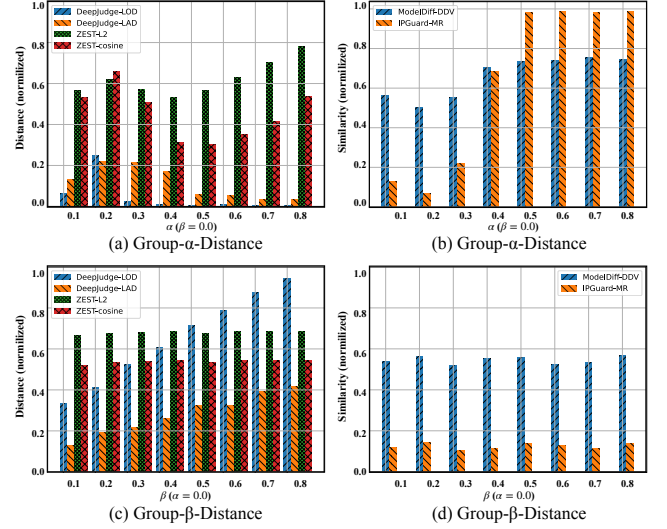


Fig. 8. Performance change of REMOVALNET with different ratios of  $\alpha$  and  $\beta$  on CIFAR10. The results are averaged with ten created surrogate models.

CelebA. Figure 7 depicts the learning curves of KnockoffNets (solid green and red lines) and the average accuracies of REMOVALNET (dashed blue and orange lines) on VGG19. We can observe from Figure 7 that, in the CelebA+31 dataset, KnockoffNets uses nearly 2000 ~ 3000 iterations to achieve a fidelity comparable to REMOVALNET ( $\times 2$  times higher than REMOVALNET). Even worse, the training overhead of KnockoffNets reaches 6000 ~ 8000 iterations in the CIFAR10, which is nearly  $\times 7$  times higher than REMOVALNET. Overall, the REMOVALNET is computational efficiency that it can save 50 ~ 85% of computational resources compared with advanced model stealing attacks.

## 4.5 Ablation Study

In this section, we discuss two impacts of REMOVALNET (i.e., the impact of latent-level and logits-level removal) and explain two phenomena of REMOVALNET including the visualization of the activated feature maps and decision boundary.

### 4.5.1 Impacts of the latent-level and logits-level removal.

As mentioned in Section 3, the DNN fingerprint removal procedure is conducted on the latent-level and logits-level, which are controlled by  $\alpha$  and  $\beta$ . Specifically, the  $1 - \alpha$  controls the KL-divergence loss,  $\alpha$  controls the cross-entropy loss, and the  $\beta$  controls the  $\mathcal{L}_{feat}$ . In this experiment, we set the learning rate to 0.03. When evaluating the impact of  $\alpha$ , we set  $\beta = 0$ , and vice versa. Figure 8 (a) and (b) depict the distance and similarity score of REMOVALNET with various  $\alpha$ . We can observe from subfigures (a) and (b) that with the  $\alpha$  increasing, the metrics of ZEST, ModelDiff, and IPGuard gradually grow. In contrast, the influence of  $\alpha$  on DeepJudge’s performance remains relatively minor. The experimental results indicate that large  $\alpha$  is better for ZEST, while small  $\alpha$  is better for ModelDiff and IPGuard. This is because a larger cross-entropy constraint leads to greater similarity between the surrogate and victim models within

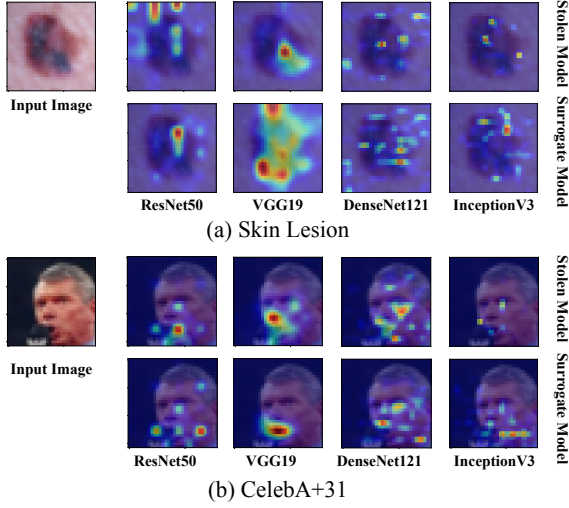


Fig. 9. Examples of saliency maps for Layer#2 of the victim model and surrogate model generated by LayerCAM [46].

the decision boundary. Figure 8 (c) and (d) depict the performance of REMOVALNET with various  $\beta$ . We can observe from subfigures (c) and (d) that the results of REMOVALNET on DeepJudge progressively rise with the growing  $\beta$ . In contrast, the impact of  $\beta$  on the performance of ZEST, ModelDiff, and IPGuard remains comparatively negligible. This is because the influence of latent-level removal on the decision boundary is small, leading to only small changes in performance on ZEST, ModelDiff, and IPGuard.

4.5.2 Visualization of saliency maps.

The saliency maps provide a technique to explore the hidden layers of CNN, which can be used to interpret the behavior of a deep neural network. In this section, we employ the LayerCAM [46] to produce reliable class activation maps (i.e., the saliency maps) to show the behavioral patterns changes of the surrogate model in the hidden layers. To facilitate a more comprehensive comparison, we perform our attack on four distinct network architectures in order to demonstrate variations in saliency maps. Figure 9 exhibits the heatmap visualization of the class activation maps on the Skin Lesion and CelebA+31 datasets. In the first and second rows of Figure 9, the heatmap highlights the activated areas of the victim and surrogate models. We can observe that the activated areas are remarkably different between the target and surrogate models. The reason behind this phenomenon is that the min-max bilevel optimization distills the knowledge of the victim model, accompanied by maximizing the distance of feature maps between the victim model and surrogate models. In general, the REMOVALNET is capable of removing the behavioral patterns in the latent representations by activating different neurons.

4.5.3 Visualization of the decision boundary.

Figure 10 depicts the decision boundary changes of the surrogate model of REMOVALNET trained on CIFAR10. We randomly select 100 test samples for each class and exploit T-SNE to embed the output probabilities of the surrogate and victim models. We can observe from Figure 10 that the outputs of the surrogate model overlap with that of

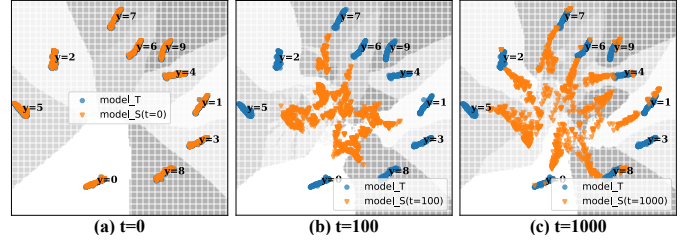


Fig. 10. Decision boundary changes of the surrogate model  $F_S$  on CIFAR10.

the victim model at the beginning. After 100 iteration optimization, the outputs of the surrogate model move into the center of the coordinate, and the output difference becomes obfuscated. Finally, after 1000 iterations, the decision boundary of the surrogate model becomes significantly different from the victim model. Figure 10 demonstrates that the DNN fingerprint removal over the logits-level changes the behavioral patterns of the victim model over the decision boundary.

5 DISCUSSIONS

5.1 Possible Countermeasures

**Adversarial attacks [20].** Chen *et al.* propose a model distance metric, called *Robustness Distance (RobD)*, to measure the robustness distance between the victim and suspected models [20]. RobD’s core insight is that a model’s robustness (Rob) is linked to the decision boundary, while the decision boundary is learned by a unique optimization process. Generally, robustness is a property of DNN, which comes from the non-robustness features in training data [47]. Therefore, injecting non-robustness features during training can promote the robustness distance between the victim and surrogate models. In fact, the removal process introduces noise variation into the latent representations, which are non-robust features. However, injecting excessive non-robust features will inevitably injure the robustness of the surrogate model. Ultimately, our main concern should be the adverse impact of DNN fingerprint removal, which can make the surrogate model more vulnerable to adversarial attacks.

TABLE 4 Performance of the potential countermeasure on CIFAR10.  $RobD_{F_S}$  denotes the RobD between  $F_V$  and  $F_S$ .

| Metric \ Method | $Rob_{F_V}$  | $Rob_{F_S}$  | $Rob_{Neg}$ | $RobD_{F_S}$ | $RobD_{Neg}$ |
|-----------------|--------------|--------------|-------------|--------------|--------------|
| FGSM            | 0.694        | 0.553        | 0.599       | 0.141        | 0.095        |
| PGD             | 0.501        | 0.422        | 0.419       | <u>0.079</u> | <u>0.083</u> |
| DeepFool        | <u>0.070</u> | <u>0.171</u> | 0.121       | 0.101        | 0.051        |

**Evaluation.** In this context, we use Rob and RobD metrics to investigate the feasibility of the adversarial attacks on the CIFAR10 dataset. The Rob is defined as its fidelity on adversarial set  $\mathcal{D}_{adv}$ :

$$Rob(F_V, \mathcal{D}_{adv}) = \frac{1}{|\mathcal{D}_{adv}|} \sum_{(x_i, y_i) \in \mathcal{D}_{adv}} \mathbb{1}[F_V(x_i) = y_i] \quad (16)$$

Furthermore, the robustness distance between the victim and surrogate models is defined as:

$$RobD(F_V, F_S, \mathcal{D}_{adv}) = |Rob(F_V, \mathcal{D}_{adv}) - Rob(F_S, \mathcal{D}_{adv})| \quad (17)$$

We report the results of Rob and RobD against FGSM, PGD, and DeepFool in Table 4. As illustrated in Table 4, (1) both the target, surrogate, and negative models are not robust to adversarial attacks, (2) the surrogate model's robustness drops in FGSM and PGD but has a small increase in DeepFool (i.e.,  $Rob_{F_V} = 0.07$  vs  $Rob_{F_S} = 0.171$ ), and (3) for the PGD attack,  $RobD_{F_S} = 0.079$  is close to  $RobD_{F_V} = 0.083$ , meaning it's difficult only to use RobD to determine whether a suspected model is a copy of the victim model.

**Dataset inference [48].** Dataset inference is a novel DNN ownership verification technique that identifies whether a suspected model has private knowledge from the victim model's dataset. This approach leverages the insight that knowledge contained in the victim model's training set is commonly shared among all stolen replicas. Consequently, dataset inference demonstrates resilience in detecting surrogate models derived from the victim model. To circumvent this technique, an adversary should remove the semantic knowledge embedded within the surrogate model. However, this action could also compromise the fidelity of the DNN model. Hence, dataset inference may be a promising direction for the research community to mitigate the DNN fingerprint removal attack.

## 5.2 Limitations and Future Work

**Evaluation on various tasks.** In this paper, we concentrate on computer vision tasks while we acknowledge that models from various domains, such as natural language processing [49], [50] and graph neural networks [51], [52], also hold significant privacy and copyright value. Notably, the transformers of pre-trained language models (e.g., LLaMA and GPT) possess a considerable capacity for embedding non-robustness features. Moreover, the powerful feature extractor of graph neural networks also can be used to remove fingerprint-specific knowledge. As such, we believe that the REMOVALNET can be adapted to these tasks. In our future endeavors, we plan to extend REMOVALNET to language and graph models.

# 6 RELATED WORKS

## 6.1 DNN Fingerprint Removal Attacks

Despite the availability of general-purpose schemes, there is currently no effective attack specifically designed for removing DNN fingerprints. In this paper, we consider the model fine-tuning, weight pruning, and distillation as the baseline of our method. Furthermore, we discuss the distinctions between DNN fingerprint removal attacks and model stealing attacks.

**Model fine-tuning.** Model fine-tuning [53] is a machine-learning method that transfer the knowledge of a victim model to a surrogate model. The most common way of fine-tuning is to reuse the feature extraction module of the victim model and retrain the classification layers.

**Model compression.** Model pruning [54] is a model compression technique that discards the model weights while maintaining its classification performance. The typical model pruning algorithm includes three phases: model training, weight pruning, and fine-tuning. Through specific criteria, the redundant weights are pruned, while the valuable weights will be kept to maintain the model performance. Knowledge distillation [55] is another model compression technique that transfers knowledge from a victim model to create a surrogate model.

**Model stealing.** In model stealing attacks, the adversary queries the victim model using substitute data and leverages the data labeled by the victim model to create his surrogate model. JBA [56] and Knockoff [45] are two generic model stealing attacks.

## 6.2 DNN Fingerprinting

DNN fingerprinting is an ownership verification technique that protects the intellectual property of the DNN model owner. DNN fingerprinting relies on the intrinsic characteristics of the neural networks to verify whether a suspected model is a copy of the victim model. Those characteristics can be represented by a sequence of behavioral patterns in the latent representations and decision boundary.

Recent works focus on investigating many metrics to measure the distance or similarity between the victim and suspected models. Existing works on DNN fingerprinting can be categorized into the white-box [20] and black-box methods [18], [19], [21], [22], [23], [24], [48], [57]. For the white-box methods, the verifier is assumed to access the intermediate layers of the suspected model. The authors of DeepJudge [20] propose multiple metrics (e.g., Layer Outputs Distance, Layer Activation Distance) to measure the distance of intermediate layers between the victim and suspected models. On the other hand, in black-box methods, the verifier only can query the suspected model with probing samples and observe its posterior probabilities. For example, the authors of [18] propose IPGuard, which extracts plenty of adversarial examples near the decision boundary of the victim model. Compared with the victim model, once the suspected model has similar responses to the extracted adversarial examples (i.e., matching rate), the suspected model is determined as a copy of the victim model. The authors of [23] propose ModelDiff, which inspects the behavioral patterns of a suspected model using the DDV. The ModelDiff outputs a similarity score to measure the behavioral patterns similarity of two models over the decision boundary. Besides, the authors of [17] adopt Universal Adversarial Perturbations (UAPs) as fingerprints to verify the copyright of the DNN model. Different from the aforementioned methods, the authors of [19], [22], [24] first generate many negative models and positive models, then employ those models as training data to generate adversarial examples. The objective of those methods is to find out conferrable adversarial examples which exclusively transfer a target label from the victim model to the surrogate model. Finally, the fidelity of the suspected model on those adversarial examples is used to determine whether the suspected model is a copy of the victim model.

## 7 CONCLUSIONS

This paper presents the first comprehensive investigation of DNN fingerprint removal attacks. We provided analytical and empirical evidence for the feasibility of the DNN fingerprint removal attack. In particular, we propose a bilevel optimization-based DNN fingerprint removal attack named REMOVALNET. We conduct extensive experiments to evaluate the **fidelity**, **effectiveness**, and **efficiency** of REMOVALNET, covering five benchmark datasets and four diverse scenarios, namely, traffic sign recognition, disease diagnosis, face recognition, and large-scale visual recognition. Our findings reveal significant threats to the verification of DNN ownership and highlight the urgent need for robust copyright protection methods, particularly against DNN fingerprint removal attacks. We hope this work can serve as a wake-up call to the dangers posed by these types of attacks and motivate the scientific community to come up with robust measures to protect against them.

## REFERENCES

- [1] K. Simonyan and A. Zisserman, "Very deep convolutional networks for large-scale image recognition," *arXiv preprint arXiv:1409.1556*, 2014.
- [2] A. Brock, S. De, S. L. Smith, and K. Simonyan, "High-performance large-scale image recognition without normalization," in *International Conference on Machine Learning*. PMLR, 2021, pp. 1059–1071.
- [3] J. DeYoung, S. Jain, N. F. Rajani, E. Lehman, C. Xiong, R. Socher, and B. C. Wallace, "ERASER: A benchmark to evaluate rationalized NLP models," in *Proceedings of the 58th Annual Meeting of the Association for Computational Linguistics, ACL 2020, Online, July 5-10, 2020*, D. Jurafsky, J. Chai, N. Schluter, and J. R. Tetraault, Eds. Association for Computational Linguistics, 2020, pp. 4443–4458.
- [4] J. Bragg, A. Cohan, K. Lo, and I. Beltagy, "Flex: Unifying evaluation for few-shot nlp," *Advances in Neural Information Processing Systems*, vol. 34, pp. 15 787–15 800, 2021.
- [5] F. Shi and Y.-F. Li, "Rapid performance gain through active model reuse," in *IJCAI*, 2019, pp. 3404–3410.
- [6] X.-Z. Wu, S. Liu, and Z.-H. Zhou, "Heterogeneous model reuse via optimizing multiparty multiclass margin," in *International Conference on Machine Learning*. PMLR, 2019, pp. 6840–6849.
- [7] J.-J. Shao, Z. Cheng, Y.-F. Li, and S. Pu, "Towards robust model reuse in the presence of latent domains," in *IJCAI*, 2021, pp. 2957–2963.
- [8] H. Yao, Z. Li, H. Weng, F. Xue, K. Ren, and Z. Qin, "Fdinet: Protecting against dnn model extraction via feature distortion index," *arXiv preprint arXiv:2306.11338*, 2023.
- [9] Y. Uchida, Y. Nagai, S. Sakazawa, and S. Satoh, "Embedding watermarks into deep neural networks," in *Proceedings of the 2017 ACM on international conference on multimedia retrieval*, 2017, pp. 269–277.
- [10] J. Zhang, Z. Gu, J. Jang, H. Wu, M. P. Stoecklin, H. Huang, and I. Molloy, "Protecting intellectual property of deep neural networks with watermarking," in *Proceedings of the 2018 on Asia Conference on Computer and Communications Security*, 2018, pp. 159–172.
- [11] Y. Adi, C. Baum, M. Cisse, B. Pinkas, and J. Keshet, "Turning your weakness into a strength: Watermarking deep neural networks by backdooring," in *27th USENIX Security Symposium (USENIX Security 18)*, 2018, pp. 1615–1631.
- [12] B. Darvish Rouhani, H. Chen, and F. Koushanfar, "Deepsigns: An end-to-end watermarking framework for ownership protection of deep neural networks," in *Proceedings of the Twenty-Fourth International Conference on Architectural Support for Programming Languages and Operating Systems*, 2019, pp. 485–497.
- [13] M. Shafieinejad, N. Lukas, J. Wang, X. Li, and F. Kerschbaum, "On the robustness of backdoor-based watermarking in deep neural networks," in *IH&MMSec '21: ACM Workshop on Information Hiding and Multimedia Security, Virtual Event, Belgium, June, 22-25, 2021*, D. Borghys, P. Bas, L. Verdoliva, T. Pevný, B. Li, and J. Newman, Eds. ACM, 2021, pp. 177–188.
- [14] N. Lukas, E. Jiang, X. Li, and F. Kerschbaum, "Sok: How robust is image classification deep neural network watermarking?" in *2022 IEEE Symposium on Security and Privacy (SP)*. IEEE, 2022, pp. 787–804.
- [15] H. Yao, J. Lou, K. Ren, and Z. Qin, "Promptcare: Prompt copyright protection by watermark injection and verification," *arXiv preprint arXiv:2308.02816*, 2023.
- [16] S. Wang and C.-H. Chang, "Fingerprinting deep neural networks—a deepfool approach," in *2021 IEEE International Symposium on Circuits and Systems (ISCAS)*. IEEE, 2021, pp. 1–5.
- [17] Z. Peng, S. Li, G. Chen, C. Zhang, H. Zhu, and M. Xue, "Fingerprinting deep neural networks globally via universal adversarial perturbations," in *Proceedings of the IEEE/CVF Conference on Computer Vision and Pattern Recognition*, 2022, pp. 13 430–13 439.
- [18] X. Cao, J. Jia, and N. Z. Gong, "Ippguard: Protecting intellectual property of deep neural networks via fingerprinting the classification boundary," in *Proceedings of the 2021 ACM Asia Conference on Computer and Communications Security*, 2021, pp. 14–25.
- [19] X. Pan, Y. Yan, M. Zhang, and M. Yang, "Metav: A meta-verifier approach to task-agnostic model fingerprinting," in *Proceedings of the 28th ACM SIGKDD Conference on Knowledge Discovery and Data Mining*, 2022, pp. 1327–1336.
- [20] J. Chen, J. Wang, T. Peng, Y. Sun, P. Cheng, S. Ji, X. Ma, B. Li, and D. Song, "Copy, right? a testing framework for copyright protection of deep learning models," in *2022 IEEE Symposium on Security and Privacy (SP)*. IEEE, 2022, pp. 824–841.
- [21] H. Jia, H. Chen, J. Guan, A. S. Shamsabadi, and N. Papernot, "A zest of lime: Towards architecture-independent model distances," in *International Conference on Learning Representations*, 2021.
- [22] N. Lukas, Y. Zhang, and F. Kerschbaum, "Deep neural network fingerprinting by conferrable adversarial examples," in *9th International Conference on Learning Representations, ICLR 2021, Virtual Event, Austria, May 3-7, 2021*. OpenReview.net, 2021.
- [23] Y. Li, Z. Zhang, B. Liu, Z. Yang, and Y. Liu, "Modeldiff: testing-based dnn similarity comparison for model reuse detection," in *Proceedings of the 30th ACM SIGSOFT International Symposium on Software Testing and Analysis*, 2021, pp. 139–151.
- [24] K. Yang, R. Wang, and L. Wang, "Metafinger: Fingerprinting the deep neural networks with meta-training," in *Proceedings of the Thirty-First International Joint Conference on Artificial Intelligence, IJCAI 2022, Vienna, Austria, 23-29 July 2022*, L. D. Raedt, Ed. ijcai.org, 2022, pp. 776–782.
- [25] X. Cun and C.-M. Pun, "Split then refine: stacked attention-guided resnets for blind single image visible watermark removal," in *Proceedings of the AAAI Conference on Artificial Intelligence*, vol. 35, no. 2, 2021, pp. 1184–1192.
- [26] X. Chen, W. Wang, C. Bender, Y. Ding, R. Jia, B. Li, and D. Song, "Refit: a unified watermark removal framework for deep learning systems with limited data," in *Proceedings of the 2021 ACM Asia Conference on Computer and Communications Security*, 2021, pp. 321–335.
- [27] T. Wang and F. Kerschbaum, "Riga: Covert and robust white-box watermarking of deep neural networks," in *Proceedings of the Web Conference 2021*, 2021, pp. 993–1004.
- [28] Q. Zhong, L. Y. Zhang, S. Hu, L. Gao, J. Zhang, and Y. Xiang, "Attention distraction: Watermark removal through continual learning with selective forgetting," in *IEEE International Conference on Multimedia and Expo, ICME 2022, Taipei, Taiwan, July 18-22, 2022*. IEEE, 2022, pp. 1–6.
- [29] J. Ye, Y. Fu, J. Song, X. Yang, S. Liu, X. Jin, M. Song, and X. Wang, "Learning with recoverable forgetting," in *Computer Vision—ECCV 2022: 17th European Conference, Tel Aviv, Israel, October 23–27, 2022, Proceedings, Part XI*. Springer, 2022, pp. 87–103.
- [30] M. T. Ribeiro, S. Singh, and C. Guestrin, "Why should i trust you?" explaining the predictions of any classifier," in *Proceedings of the 22nd ACM SIGKDD international conference on knowledge discovery and data mining*, 2016, pp. 1135–1144.
- [31] S. Guo, T. Zhang, H. Qiu, Y. Zeng, T. Xiang, and Y. Liu, "Fine-tuning is not enough: A simple yet effective watermark removal attack for dnn models," *arXiv preprint arXiv:2009.08697*, 2020.
- [32] K. Pei, Y. Cao, J. Yang, and S. Jana, "Deepxplore: Automated whitebox testing of deep learning systems," in *proceedings of the 26th Symposium on Operating Systems Principles*, 2017, pp. 1–18.
- [33] A. Mallya and S. Lazebnik, "Packnet: Adding multiple tasks to a single network by iterative pruning," in *Proceedings of the IEEE conference on Computer Vision and Pattern Recognition*, 2018, pp. 7765–7773.

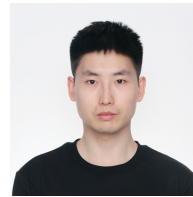
- [34] J. Rajasegaran, M. Hayat, S. Khan, F. S. Khan, and L. Shao, "Random path selection for incremental learning," *Advances in Neural Information Processing Systems*, vol. 3, 2019.
- [35] A. Krizhevsky, G. Hinton *et al.*, "Learning multiple layers of features from tiny images," 2009.
- [36] J. Stallkamp, M. Schlupsing, J. Salmen, and C. Igel, "Man vs. computer: Benchmarking machine learning algorithms for traffic sign recognition," *Neural networks*, vol. 32, pp. 323–332, 2012.
- [37] N. Codella, V. Rotemberg, P. Tschandl, M. E. Celebi, S. Dusza, D. Gutman, B. Helba, A. Kallou, K. Liopyris, M. Marchetti *et al.*, "Skin lesion analysis toward melanoma detection 2018: A challenge hosted by the international skin imaging collaboration (isic)," *arXiv preprint arXiv:1902.03368*, 2019.
- [38] Z. Liu, P. Luo, X. Wang, and X. Tang, "Large-scale celebfaces attributes (celeba) dataset," *Retrieved August*, vol. 15, no. 2018, p. 11, 2018.
- [39] O. Russakovsky, J. Deng, H. Su, J. Krause, S. Satheesh, S. Ma, Z. Huang, A. Karpathy, A. Khosla, M. Bernstein *et al.*, "Imagenet large scale visual recognition challenge," *International journal of computer vision*, vol. 115, no. 3, pp. 211–252, 2015.
- [40] L. N. Darlow, E. J. Crowley, A. Antoniou, and A. J. Storkey, "Cinic-10 is not imagenet or cifar-10," *arXiv preprint arXiv:1810.03505*, 2018.
- [41] G. B. Huang, M. Mattar, T. Berg, and E. Learned-Miller, "Labeled faces in the wild: A database for studying face recognition in unconstrained environments," in *Workshop on faces in Real-Life Images: detection, alignment, and recognition*, 2008.
- [42] Q. Cao, L. Shen, W. Xie, O. M. Parkhi, and A. Zisserman, "Vg-gface2: A dataset for recognising faces across pose and age," in *2018 13th IEEE international conference on automatic face & gesture recognition (FG 2018)*. IEEE, 2018, pp. 67–74.
- [43] M. Combalia, N. C. Codella, V. Rotemberg, B. Helba, V. Vilaplana, O. Reiter, C. Carrera, A. Barreiro, A. C. Halpern, S. Puig *et al.*, "Bcn20000: Dermoscopic lesions in the wild," *arXiv preprint arXiv:1908.02288*, 2019.
- [44] G. Menardi and N. Torelli, "Training and assessing classification rules with imbalanced data," *Data mining and knowledge discovery*, vol. 28, no. 1, pp. 92–122, 2014.
- [45] T. Orekondy, B. Schiele, and M. Fritz, "Knockoff nets: Stealing functionality of black-box models," in *Proceedings of the IEEE/CVF conference on computer vision and pattern recognition*, 2019, pp. 4954–4963.
- [46] P.-T. Jiang, C.-B. Zhang, Q. Hou, M.-M. Cheng, and Y. Wei, "Layercam: Exploring hierarchical class activation maps for localization," *IEEE Transactions on Image Processing*, vol. 30, pp. 5875–5888, 2021.
- [47] A. Ilyas, S. Santurkar, D. Tsipras, L. Engstrom, B. Tran, and A. Madry, "Adversarial examples are not bugs, they are features," in *Advances in Neural Information Processing Systems 32: Annual Conference on Neural Information Processing Systems 2019, NeurIPS 2019, December 8-14, 2019, Vancouver, BC, Canada*, H. M. Wallach, H. Larochelle, A. Beygelzimer, F. d'Alché-Buc, E. B. Fox, and R. Garnett, Eds., 2019, pp. 125–136.
- [48] P. Maini, M. Yaghini, and N. Papernot, "Dataset inference: Ownership resolution in machine learning," in *9th International Conference on Learning Representations, ICLR 2021, Virtual Event, Austria, May 3-7, 2021*, 2021.
- [49] H. Touvron, L. Martin, K. Stone, P. Albert, A. Almahairi, Y. Babaei, N. Bashlykov, S. Batra, P. Bhargava, S. Bhosale *et al.*, "Llama 2: Open foundation and fine-tuned chat models," *arXiv preprint arXiv:2307.09288*, 2023.
- [50] T. Brown, B. Mann, N. Ryder, M. Subbiah, J. D. Kaplan, P. Dhariwal, A. Neelakantan, P. Shyam, G. Sastry, A. Askell *et al.*, "Language models are few-shot learners," *Advances in neural information processing systems*, vol. 33, pp. 1877–1901, 2020.
- [51] B. Wu, X. Yang, S. Pan, and X. Yuan, "Model extraction attacks on graph neural networks: Taxonomy and realisation," in *Proceedings of the 2022 ACM on Asia Conference on Computer and Communications Security*, 2022, pp. 337–350.
- [52] H. Zhang, B. Wu, X. Yuan, S. Pan, H. Tong, and J. Pei, "Trustworthy graph neural networks: Aspects, methods and trends," *arXiv preprint arXiv:2205.07424*, 2022.
- [53] Y. Guo, H. Shi, A. Kumar, K. Grauman, T. Rosing, and R. Feris, "Spottune: transfer learning through adaptive fine-tuning," in *Proceedings of the IEEE/CVF conference on computer vision and pattern recognition*, 2019, pp. 4805–4814.
- [54] Z. Liu, M. Sun, T. Zhou, G. Huang, and T. Darrell, "Rethinking the value of network pruning," in *7th International Conference on*

*Learning Representations, ICLR 2019, New Orleans, LA, USA, May 6-9, 2019*. OpenReview.net, 2019.

- [55] J. Gou, B. Yu, S. J. Maybank, and D. Tao, "Knowledge distillation: A survey," *International Journal of Computer Vision*, vol. 129, no. 6, pp. 1789–1819, 2021.
- [56] N. Papernot, P. McDaniel, I. Goodfellow, S. Jha, Z. B. Celik, and A. Swami, "Practical black-box attacks against machine learning," in *Proceedings of the 2017 ACM on Asia conference on computer and communications security*, 2017, pp. 506–519.
- [57] Z. Zhang, Y. Li, J. Wang, B. Liu, D. Li, Y. Guo, X. Chen, and Y. Liu, "Remos: reducing defect inheritance in transfer learning via relevant model slicing," in *Proceedings of the 44th International Conference on Software Engineering*, 2022, pp. 1856–1868.



**Hongwei Yao** is currently a Ph.D. student at the College of Computer Science and Technology, Zhejiang University, advised by Dr. Zhan Qin. Prior to that, he obtained his bachelor (2016) and master (2020) degrees from Hangzhou Dianzi University. His research focuses on machine learning security and privacy.



**Zheng Li** is currently a Ph.D. student at CISPA Helmholtz Center for Information Security, advised by Dr. Yang Zhang. Prior to that, he obtained his bachelor (2017) and master (2020) degrees from Shandong University under the supervision of Prof. Shanjing Guo. His research focuses on machine learning security and privacy.



**Kunzhe Huang** received the B.S. degree from the Department of Computer Science and Engineering, Central South University, in 2019. He is a graduate student at the Department of Computer Science and Technology, Zhejiang University. His research interests include security and privacy in deep learning.



**Jian Lou** is currently a researcher at Hangzhou Innovation Center at Zhejiang University. He was an associate professor at Xidian University from 2021 to 2022. He was a Post-doc in the Department of Computer Science at Emory University from 2019 to 2021. He obtained Ph.D. in Computer Science at Hong Kong Baptist University in 2018. Prior to that, He received a B.S. in Mathematics from Zhejiang University in 2013.



**Zhan Qin** is currently a ZJU100 Young Professor, with both the College of Computer Science and Technology and the Institute of Cyberspace Research (ICSR) at Zhejiang University, China. He was an assistant professor at the Department of Electrical and Computer Engineering in the University of Texas at San Antonio after receiving the Ph.D. degree from the Computer Science and Engineering department at State University of New York at Buffalo in 2017. His current research interests include data security

and privacy, secure computation outsourcing, artificial intelligence security, and cyber-physical security in the context of the Internet of Things. His works explore and develop novel security sensitive algorithms and protocols for computation and communication on the general context of Cloud and Internet devices.



**Kui Ren** is a Professor and the Dean of School of Cyber Science and Technology at Zhejiang University. Before that, he was SUNY Empire Innovation Professor at State University of New York at Buffalo. He received his PhD degree in Electrical and Computer Engineering from Worcester Polytechnic Institute. Kui's current research interests include Data Security, IoT Security, AI Security, and Privacy. He received Guohua Distinguished Scholar Award from ZJU in 2020, IEEE CISTC Technical Recognition Award

in 2017, SUNY Chancellor's Research Excellence Award in 2017, Sigma Xi Research Excellence Award in 2012 and NSF CAREER Award in 2011. Kui has published extensively in peer-reviewed journals and conferences and received the Test-of-time Paper Award from IEEE INFOCOM and many Best Paper Awards from IEEE and ACM including MobiSys'20, ICDCS'20, Globecom'19, ASIACCS'18, ICDCS'17, etc. His h-index is 74, and his total publication citation exceeds 32,000 according to Google Scholar. He is a frequent reviewer for funding agencies internationally and serves on the editorial boards of many IEEE and ACM journals. He currently serves as Chair of SIGSAC of ACM China. He is a Fellow of IEEE, a Fellow of ACM and a Clarivate Highly-Cited Researcher.